Research Article

Ammar F. Abdulwahid, Zaid S. Kareem, Hyder H. Balla*, Noora A. Hashim and Luay H. Abbud

CuO–Cu/water hybrid nonofluid potentials in impingement jet

https://doi.org/10.1515/eng-2022-0350
received May 14, 2022; accepted June 25, 2022

Abstract: The present study considered an impingement jet using hybrid nanofluid CuO–Cu/water. A single rounded nozzle was used to impinge a turbulent coolant (water) on the hot circular plate at Reynold's number range of (5,000–15,000). CuO–Cu nanoparticles were physically synthesized at 50 nm size and dispersed by one-step preparation method. The experimentations were conducted with nanoparticle concentrations range of (0.2–1%) by volume. The results showed that the presence of hybrid nanoparticles exhibits a significant improvement in the overall thermal performance of the working fluid. Where the gained heat interpreted by the Nusselt number was found to be 2.8% (in comparing with deionized water) at ϕ = 1% and Re = 15,000, while the minimum gain in the heat was found to be 0.93% at ϕ = 0.2% and Re = 5,000. Furthermore, it was noted that the excessive increase in CuO–Cu nanoparticle concentration causes more pumping power consumption. Moreover, the CuO–Cu nanoparticles residual layer was found to be formed at a high CuO–Cu concentration, which acts as an insulation layer that hinders the heat exchange. It was also found that the threshold of nozzle-to-plate spacing is H = 4, before which, the heat gain is positive, and negative plummet after.

Keywords: CuO–Cu nanoparticles, nonofluid, heat transfer, enhancement, impingement jet, hybrid

1 Introduction

Nowadays, heat transfer poses a crucial field related to all aspects of civilized communities, whether in agriculture, industry, climate, and other fields. Heat transfer is simply defined as the process of transferring heat from one substance to another that is driven by the presence of temperature difference. The traditional approaches of heat transfer enhancement were scrutinized and tested thoroughly over decades and merely nothing left to investigate [1,2]. Hence, it is imperative to follow a new approach and embrace innovative techniques to override the current challenges and vouched for the upcoming challenges and demands regarding heat transfer [3–6]. The emergence of nanotechnology helps in overcome of many issues especially in the heat transfer field. The high thermal conductivity nanopowder enhances the traditional heat transfer fluid properties, where the resulting nanofluid would consist of the nanopowder suspended in the base fluid. The most important heat transfer field that required embracing nanofluid is the jet impingement due to its wide range of applications such as electronic component cooling, metal cutting, and space applications; an experimental study of heat exchanger performance by using Cu/water (0.1, 0.2, 0.3, 0.4, and 0.5 wt%) as a working fluid was conducted by Sun et al. [6]. Where the impingement jet technique was used as a cooling mean, various parameters were examined to reveal their effect on the overall thermal performance. The reported outcomes refer to the use of nanofluid causing a significant increase in thermal performance with considerable low pressure drop. Amjadian et al. [7] conducted a series of experiments by using 15–25 nm Cu_2O/water as a working fluid that impinged from the free-rounded jet. The nanoparticles concentrations were (0.03–0.07 wt%) and Reynold's number (7,330–11,082). It was found that the using of Cu_2O/water nanofluid leads to significant enhancement by 45% at nanoparticle concentration of 0.07%. Alumina\water nanofluid was used as a working fluid being impinges from a circular confined jet to hit a flat plate at Re 20,000. It was inferred that the use of nanofluid increases the heat transfer compared to water. An experimental study of single circular free jet performance was experimentally scrutinized by Sorour et al. [8] to clarify its thermal potentials. A 8 nm SiO_2\water nanofluid chose as working fluid to enhance heat transfer process. The experiments were conducted at Re of up to

* **Corresponding author: Hyder H. Balla,** Aeronautical Techniques Department, Najaf Technical Institute, Al-Furat Al-Awsat Technical University, Kufa, Najaf, Iraq, e-mail: hyderballa@atu.edu.iq
Ammar F. Abdulwahid, Zaid S. Kareem, Noora A. Hashim: Mechanical Engineering Department, Faculty of Engineering, University of Kufa, Kufa, Najaf, Iraq
Luay H. Abbud: Air Conditioning and Refrigeration Techniques Engineering, Al-Mustaqbal University College, Hillah, Iraq

Open Access. © 2022 the author(s), published by De Gruyter. This work is licensed under the Creative Commons Attribution 4.0 International License.

4,000 and volume fraction from 0 to 8.5. It was noticed from the reported outcome that the heat transfer increases as both volume fraction and Reynolds Number, where the maximum heat transfer enhancement achieved at 8.5% volume fraction is 80%. Another experimental study regarding CuO/water nanofluid was carried out by Wongcharee et al. [9]. T was aimed to reveal the effect of both nanofluid and a nozzle with imbedded twisted tape on cooling thermal performance. The study carried out at Reynold's number range of 1,600–9,400, CuO nanoparticles concentration of 0.2–0.4% by volume, H/D of 2–4, and twist ratio of employing twisted tape of 1.43–4.28. It was found that the Nusselt number increases in the case of CuO nanoparticles concentration of 0.3 and 0.4%; moreover, it was reported that the best combination is that of CuO concentration of 0.3%, H/D of 2, and twist ratio of 1.43. The high local heat transfer rate merit of the impingement jet was exploit by Li et al. [10] to investigate the Cu/water nanofluid potentials in electronics component cooling. It was found that the stable nanofluid exhibits a good improvement in heat transfer potentials, where an enhancement of 52% was gained in heat transfer coefficient at Cu nanoparticle concentration of 30%. Nguyen et al. [11] studied the thermal performance of 36 nm Al_2O_3/water nanofluid experimentally. The nozzle had a 2 mm diameter, the H/D was varied from 2 to 10, volume fraction was of 0–6%, and Reynold's number range was 3,800–88,000. The outcomes confirmed that there was an appreciable enhancement in heat transfer in most cases. while in other cases, the opposite is occurred. In addition, the highest value of heat transfer coefficient was noticed at nozzle to plate distance of 5 mm and volume fraction of 2.8%. Tie et al. [12] tested Cu/water nanofluids in a jet array (each jet has a diameter of 1.5 mm) to reveal the thermal performance of such arrangement. The Cu nanoparticles (26 nm) volume fractions was 0.17–0.64%, and the space between the jet array and the plate was H = 15 mm. It was found that the presence of metallic nanoparticle such as Cu helps in increasing the heat transfer rate.

Based on the previous literature, the nanofluid showed good behavior as a coolant fluid, so it is important to study the application of this fluid on the impinging jet under a wide range of effecting parameters. Hence, a hybrid CuO–Cu/water nanofluid was adopted for such experimentations due to the lack of literature of using such working fluid. The objective of this study is to scrutinize the hybrid CuO–Cu/water intensively in order to reveal its potential in heat transfer enhancement under wide ranges of variables.

2 Nanofluid preparation, stability, and properties

2.1 Preparation

The preparation of nanofluid should be selected and performed cautiously because there are different approaches in preparation methods, which are the one-step (proposed by Eastman et al. [13]) and the two-step (proposed by Paul et al. [14]) approaches. The current experimentation does not aim to prepare a large scale of nanofluid, which is why the one-step preparation method was followed. Furthermore, the one-step preparation procedure is fast, simple, and reliable [1]. This method is stated that the nanoparticles could be added into the base fluid gently with stirring. It is preferable to add a stabilizer for quick and better stability. The current CuO–Cu nanoparticles (Nanostructured & Amorphous Materials, Inc) of ≈50 nm size were dispersed directly in deionized water at varicose concentration range (0.1–0.5)%; thereafter, a sodium dodecylbenzene sulfonate stabilizer or (surfactant) was added [15] at five concentration (0.1–0.5)% by weight. The presence of a stabilizer helps in the elongation of suspension time [16]. In addition, it helps in preserving both the homogeneity and continuity of the resulting nanofluid composition [17]. The surfactant acts as a binder medium between both the base fluid and suspended nanoparticles, such an arrangement provides some kind of wettability in the two-phase system [18].

2.2 Stability

Since the thermophysical properties of any nanofluid are strictly relying on the morphology of the two-phase system, the latter one is depending on the nanofluid stability in return. Therefore, the stability of the prepared nanofluid is one of the prime issues in the current research to vouch for the fidelity of the expected outcomes [19]. The Brownian motion phenomenon would not be sufficient in inducing a homogeneous mixture. Accordingly, the prepared nanofluid was agitated by an ultrasonic (Sonix VCX 130, 20 kHz, 130 W) device under a 123 μm soundwave amplitude to hinder the agglomeration. The agitation process lasts one hour in a dark place and at room temperature. Scanning electron microscopy (SEM) helped in the stability verification of the nanofluid, which is the last step prior to commencing the experimentations; this step

is shown in Figure 1. It shows a good homogeneity with no clustering existence among the suspended nanoparticles; such a homogeneous mixture would be slightly affected by the gravitational effect, and hence, sedimentation would be negligible.

2.3 Properties

The thermophysical properties of the nanofluid are measured several times for each nanoparticle concentration at a temperature range (20–50)°C, and the average reading was calculated for each property. The thermal conductivity k_{nf} was measured by a reliable coded method (recommended by both IEEE442-1981 and ASTM D5334 standard). It is the KD2 Pro thermal property analyzer device that basically used the transient hot wire method for minimizing the convection effect [20]. The viscosity of the nanofluid μ_{nf} obtained by (ROTAVISC lo-vi complete, 100–240 V, IKA Viscometers, Germany) device. However, specific heat capacity was obtained with the aid of (C 6000 – IKA Laboratory calorimeter, Germany). Eventually, Ø is the volume fraction obtained by the following equation [1] (Figures 2–4):

$$\varnothing = V_{np}/(V_f + V_{np}). \quad (1)$$

3 Experimentations

3.1 Experimental setup

The current experiments are conducted in an open loop pipe system which is able to equip five liters of working fluid as shown in Figure 5.

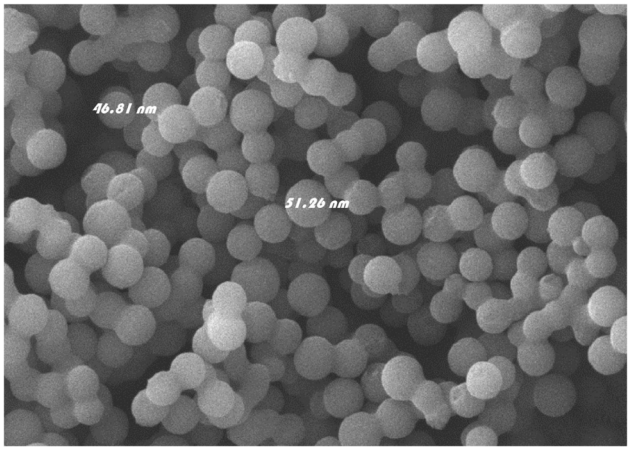

Figure 1: SEM of CuO–Cu nanofluid suspension.

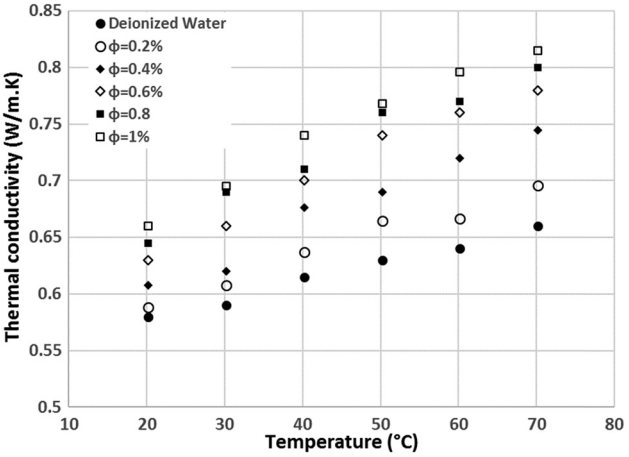

Figure 2: Thermal conductivity measurement of CuO–Cu nanofluid.

It consists of two (self-priming jet electropumps of 1.4 hp, Conforto S.r.l, Italy) gear pumps. They provide the initiation pressure to circulate the working fluid into the pie system, while the second one sucks the nanofluid from the accumulating tank toward the heat exchanger. It also contains a Control and bypass valves; a flowmeter (MR3L10SVVT, Brooks Flow meters, USA) to measure the flow rate and ensuring the exact amount of low is supplied to meet the required Reynold's number. The plenum chamber (which contains an resistance temperature detector (RTD) to measure the impinged nanofluid temperature) is located right before the brass jet nozzle (2 mm diameter), and the stainless-steel circular target plate (r = 75 mm, 6 mm thickness). Seven thermocouples (J-type) were fixed thoroughly on the back surface hot plate to read the local back-surface temperature distribution, while it is heated by a standard wire gage electric heater, which is located in a groove

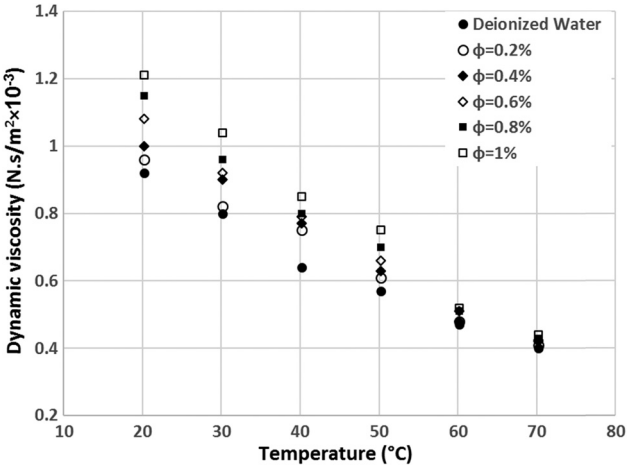

Figure 3: Dynamic viscosity measurements of CuO–Cu nanofluid.

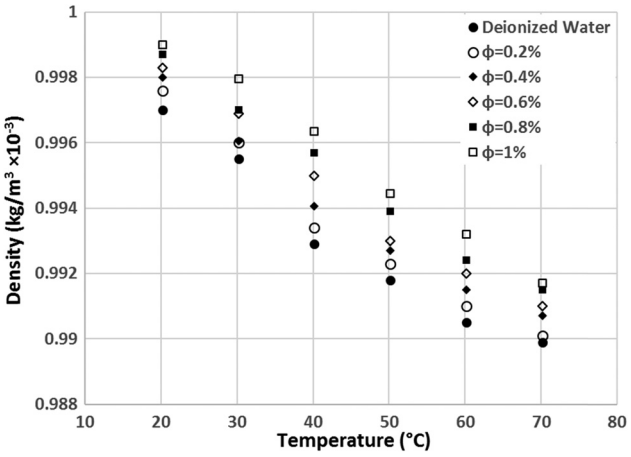

Figure 4: Density measurement of CuO–Cu nanofluid.

made in a ceramic block below the plate. A Watt Meter (Reed Instruments DW-6060 Watt Meter) was employed to measure the exact supplied energy to the SWG heater. The thermocouples and RTDs were connected to data acquisition of the reading displayed by the NI LabVIEW software package. The required supplied heat is controlled and adjusted by the voltage regulator. A Teflon case was arranged to surround the ceramic block laterally with a 20 mm gap filled by rockwool to hinder convection, conduction, and radiation. Thereafter, the nanofluid is sucked by the second pump to remove the gained heat by (SC0004 Type1, MADDEN Engineered Products, LLC) heat exchanger. Eventually, the cooled nanofluid settled in the constant temperature water bath (EW-12152-00, 25 L, 60 Hz, Stuart Shaking Water Baths, Cole-Parmer) at 25°C (±0.4°C).

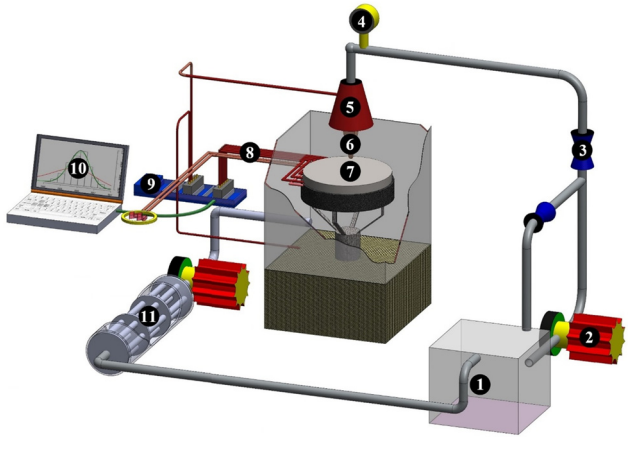

Figure 5: Experimental setup and orientations: (1) water bath, (2) pump, (3) control valve, (4) flow meter, (5) plenum chamber, (6) nozzle, (7) target plate, (8) thermocouples, (9) data accusation, and (10) heat exchanger.

3.2 Experimental procedure

Onset, the nanofluid is settled at the constant temperature water bath at ≈25°C (under low vibration) with a certain nanoparticle concentration (Ø = 0.2, 0.4, 0.6, 0.8, and 1%), and then, the first gear pump starts pushing the working fluid at the required Reynold's number (Re = 5,000, 6,000, 7,000, 8,000, 9,000, and 10,000). Reynold's number calculated by ref. [1]

$$\mathrm{Re}_{\mathrm{nf}} = \rho_{\mathrm{nf}} u D / \mu_{\mathrm{nf}}. \tag{2}$$

The D represents the inner jet diameter, and u parameter is the flow velocity which is calculated by the flow rate equation [1]

$$u = Q/(\rho_{\mathrm{nf}} a). \tag{3}$$

In the aforementioned flow rate (Q) equation, a is the pipe cross-sectional area. The required value of the working fluid flow rate was acquired by manipulating the valves at a certain position. Then, the power is switched on and the voltage regulator is adjusted to supply the required power (1,000 W) to warm the target plate. Meanwhile, the nanofluid hits the warm target plate to extract heat by convection according to the following energy balance equation [1]:

$$\dot{m} Cp(T_{\mathrm{o}} - T_i) = hA(T_{\mathrm{us}} - T_i). \tag{4}$$

In the above expression, $\dot{m}$ is the mass flow rate of the impinged nanofluid, T_i is the impinged nanofluid temperature, and T_{o} is the temperature of nanofluid after hitting the plate (nanofluid temperature at the accumulating tank), whereas h is the heat transfer coefficient which is the required parameter in the above equation. A represents plate's circular surface area. T_{us} denotes the plate's upper surface of the plate. Lastly, thirty minutes is the time out prior to taking readings into account in order to attain a steady state.

Since the thermocouples read the lower plate's temperature T_{ls}, subsequently, the T_{us} is computed by a simple one conduction equation as follows [1]:

$$q^{\cdot} = -k(T_{\mathrm{us}} - T_{\mathrm{ls}}). \tag{5}$$

The heat flux is represented by $q^{\cdot}$ ($q^{\cdot} = q/A$) in the previous equation, where the q is the supplied AC power that is adjusted by the voltage regulator and measured by Wattmeter, while k is the target plate conductivity.

Eventually, the heat transfer is often interpreted by the Nusselt number, and the last parameter was founded by the following equation:

$$\mathrm{Nu}_{\mathrm{nf}} = hD/k_{\mathrm{nf}}. \tag{6}$$

3.3 Uncertainty

The uncertainty could be reduced, but it could not perish because the uncertainty is inherited in the measuring probs a and instruments. Uncertainty is always associated with readings, and there is no measuring device without errors because human and experimental errors are anticipated. Subsequently, significant effort was paid to the current experimentation to minimize errors. Hence, a confidence level of 95% was adopted in the uncertainty analysis [21] as follows (Table 1):

$$\left(\frac{\delta \mathrm{Re}}{\mathrm{Re}}\right) = \sqrt{\left[\left(\frac{\delta U}{U}\right)^2 + \left(\frac{\delta D}{D}\right)^2 + \left(\frac{\delta \rho}{\rho}\right)^2 + \left(\frac{\delta \mu}{\mu}\right)^2\right]} \quad (7)$$

$$= 2.871\%,$$

$$\left(\frac{\delta h}{h}\right) = \sqrt{\left[\left(\frac{\delta U}{U}\right)^2 + \left(\frac{\delta D}{D}\right)^2 + \left(\frac{\delta \varnothing}{\varnothing}\right)^2 + \left(\frac{\delta T}{T}\right)^2\right]} \quad (8)$$

$$= 3.01\%,$$

$$\left(\frac{\delta \mathrm{Nu}}{\mathrm{Nu}}\right) = \sqrt{\left[\left(\frac{\delta h}{h}\right)^2 + \left(\frac{\delta D}{D}\right)^2 + \left(\frac{\delta k}{k}\right)^2\right]} = 2.44\%. \quad (9)$$

4 Results and discussions

4.1 Validation

It is often used to verify the fidelity of the adopted approaches and procedures. The experimentation would be headed in the right direction when validation shows acceptable correspondence. The current validation was conducted by mimicking the same arrangement and boundary conditions as stated by Sun et al. [22] and Wongcharee et al. [9] respectively.

Since the water was being examined over decades thoroughly, and its thermal and physical properties are well known, it was selected as a reference to be the standard measure that other fluids compared within the current study as shown in Figure 6.

The previous figure shows some divergence between the current results and the other two studies. In addition, it shows a deviation between the other two studies itself. The reason behind this deviation is the inherent uncertainties of each measuring equipment and probs. Moreover,

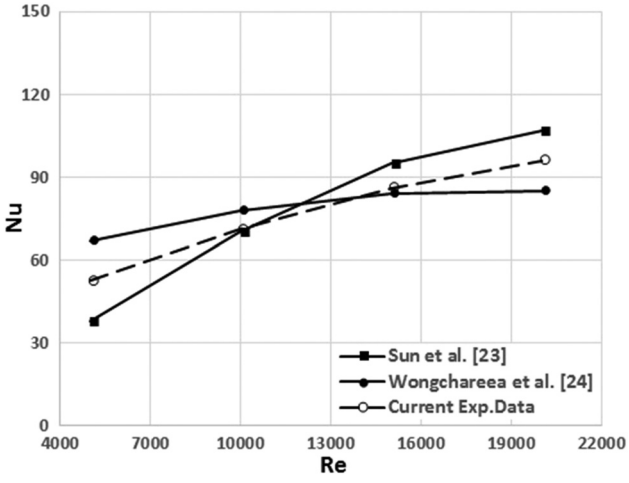

Figure 6: Current validation with both Sun et al. [22] and Wongcharee et al. [9] respectively.

Table 1: Instruments uncertainties

Item	Uncertainty	Model
Pump	±1.30%	Conforto S.r.l
Nanoparticles concentration	±0.07%	50 nm APS, MKnano
Flow Meter	±2.20%	MR3L lOSVVT, Brooks flow meters
Jet nozzle diameter	±0.08 mm	
Data acquisition	±0.6%	NI DAQ 9172
Target plate diameter	±0.1 mm	
Heating wire (0.6 m)	±1.21%	Standard Wire Gauge SWG
Wattmeter	±0.5 Watt	Reed Instruments DW-6060
Thermocouples	±0.20%	J-Type thermocouples
Temperature probe	±1.950%	Ptl OO-Type temperature probes
Voltage source	±2.30%	AYR-Voltage regulator relay
Thermal conductivity meters	±0.20%	THW-Ll ASTM D7896-19
Viscometer	±0.50%	DVl Viscometer, Brookfield Ametek
Heat exchanger	±0.34%	SC0004 Type l, MADDEN Engineered Products

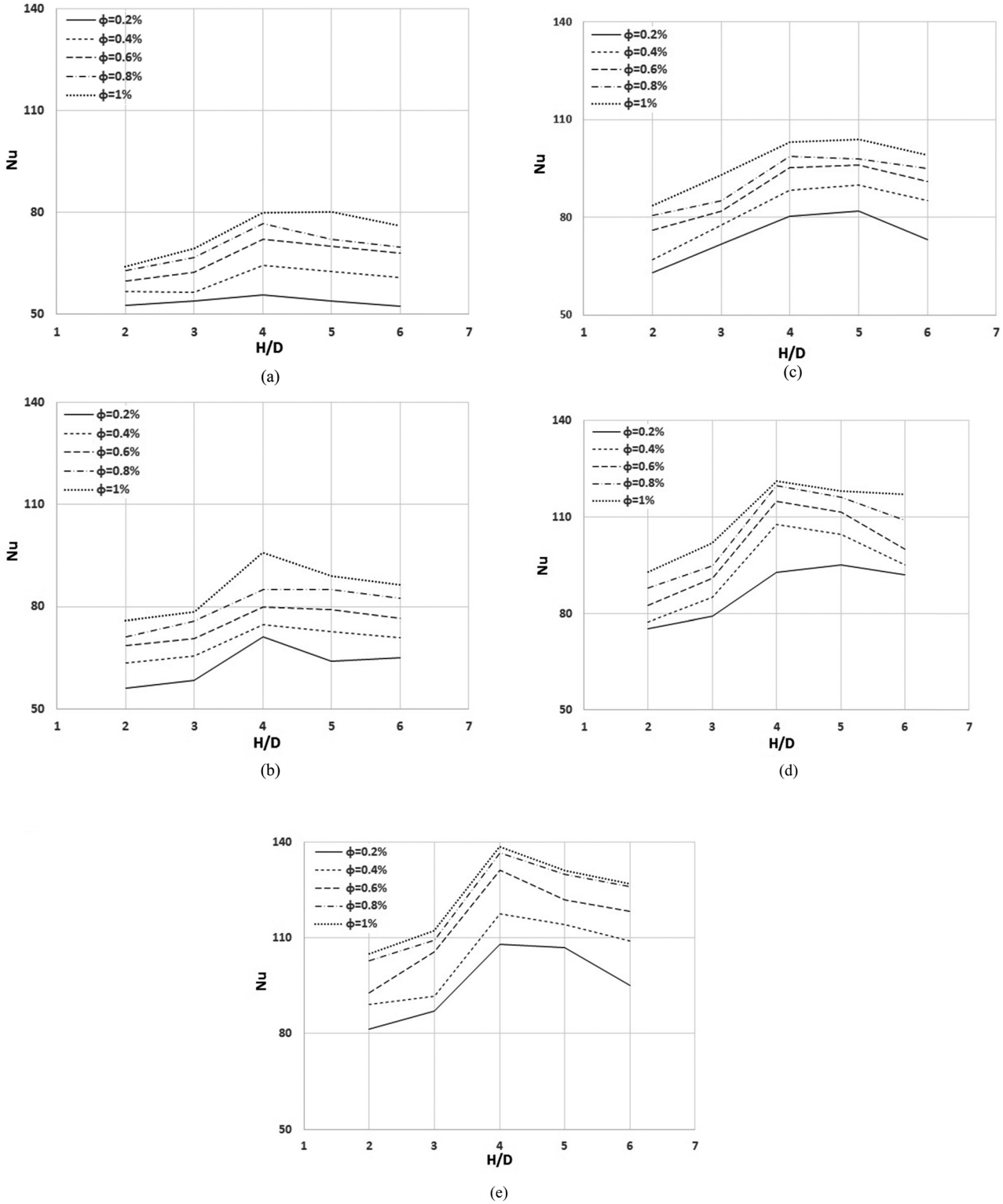

Figure 7: Nozzle-to-target plat ration effect (a) H/D = 2, (b) H/D = 3, (c) H/D = 4, (d) H/D = 5, and (e) H/D = 6 on Nusselt number.

the heat loss by convection and conduction in the current study which is estimated to be (±3%) has a share in this deviation as in the comparable two studies as well. Furthermore, the heat transfer coefficient calculation is strongly relying on thermocouples number and mounting location. As the thermocouple number increases, the reading accuracy

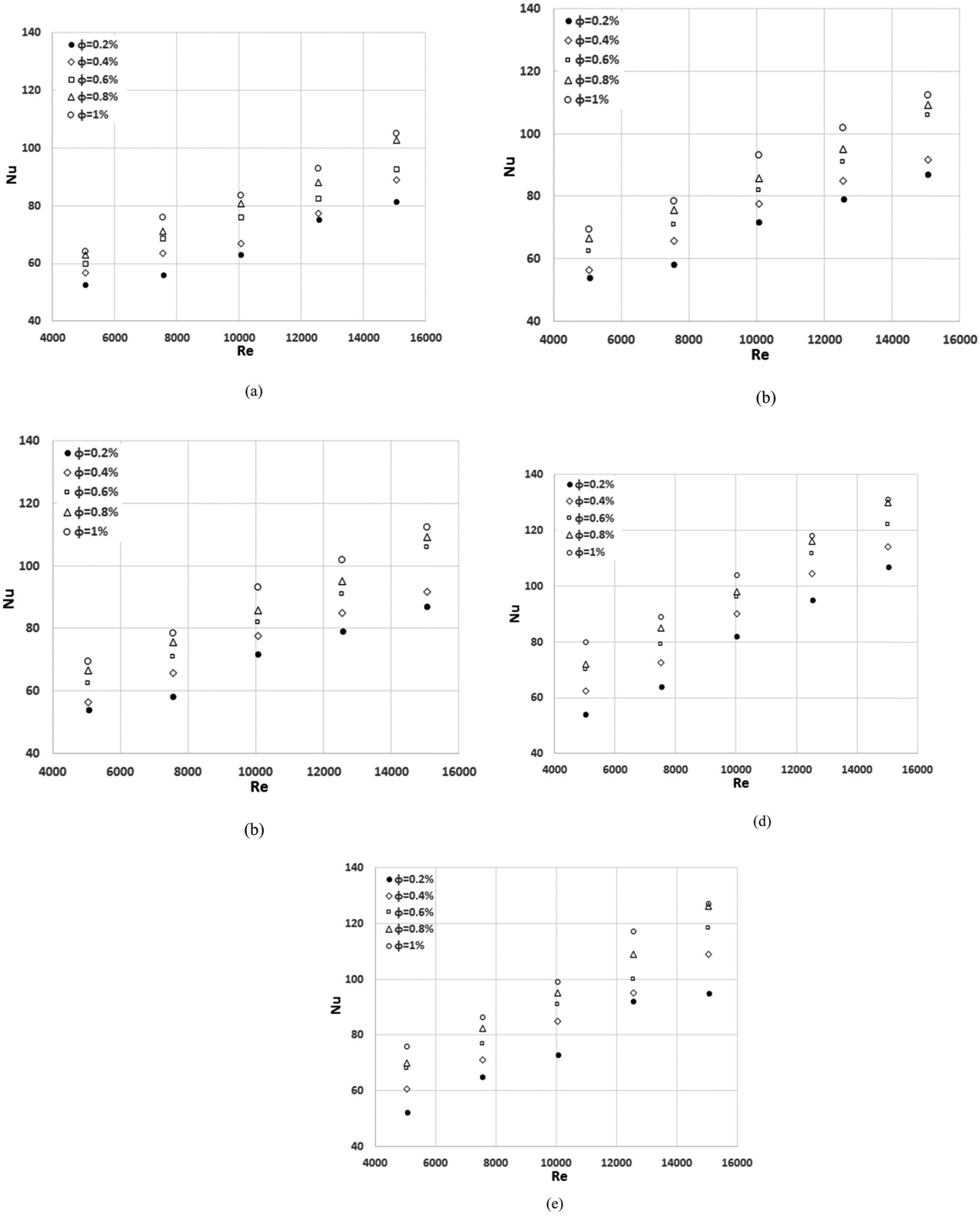

Figure 8: Nusselt number versus Reynold's number at various CuO–Cu nanoparticle concentrations, with (a) $H/D = 2$, (b) $H/D = 3$, (c) $H/D = 4$, (d) $H/D = 5$, and (e) $H/D = 6$.

increases and the average heat transfer coefficient would be closer to the right value as a result. Nevertheless, the raised deviation of (±11%) is still acceptable

4.2 Effect of (H/D) ratio

The ratio of nozzle-to-plate distance (H) to the nozzle diameter (D) has a potent effect on the heat transfer rate process between the working fluid and the hot plate, where it was found that the average Nusselt number has low values at $H/D = 2$ at all nanoparticle concentrations. These values keep on increasing as H/D increases till $H/D = 4–5$. The same trends are reported by ref. [23] and [24], where the peak was found to be 2.5–3 and 2 in both studies respectively. However, the Nusselt number attains its maximum values at this peak as shown in Figure 7.

Further increase in H/D (i.e. H/D = 6) causes a decrease in Nusselt number, which was already reported by Webb and Ma [25] and Lv et al. [26].

The reason behind this weird phenomenon is that at a small H/D value, the impinged flow was not able to be fully developed (the potential core is so close to the plate) and strikes the hot plate uniformly without mixing with the environment, i.e., uniform impingement without intense turbulence which could not break both hydraulic and thermal boundary layers.

It seems to be as the H increases, the intensity of the flow increases and the fluid impinges the plate with more energy and thrust, and this flow strength weakening the hydraulic and thermal boundary layers. As a result, more energy is exchanged.

Further increases in H/D ($H/D > 6$) cause a lateral dissipation in the flow stream of the jet, this dissipation would weaken the flow momentum, and the fluid strike the plate easily.

4.3 Nanoparticles concentration effect of CuO–Cu

In this section, the presence of metallic hybrid nanoparticle additives of CuO–Cu is considered, which is the major objective of the current stud. Figure 8(a–e) shows the Nusselt number (Nu) versus Reynold's number (Re) at various CuO–Cu/water nanofluid (nanoparticles concentrations ϕ of 0.2, 0.4, 0.6, 0.8, and 1%).

In general, and as it is commonly well known, any metallic additives (those whom having high thermal conductivity) would produce a high thermal conductivity mixture when they disperse in the most base fluid. This trend is clearly depicted in Figure 8. It shows an increase in Nusselt number as CuO–Cu nanoparticles concentration increases in the base fluid. The well-prepared and stable CuO–Cu/water nanofluid initiates thermal diffusion since they swim in the base fluid, in addition between the nanoparticle themselves by each contact. Moreover, the metallic nanoparticles exhibit a very good heat exchange when they strike the target plate more than the base fluid. These reasons are responsible directly for the gained enhancement in heat transfer. That enhancement in the Nusselt number hareached a value of 2.8% (in comparison with deionized water) at $\phi = 1\%$ and Re = 15,000, while the minimum enhancement in the Nusselt number was found to be 0.93% at $\phi = 0.2\%$ and Re = 5,000.

5 Conclusions

The present experimentations emphases on the CuO–Cu/water nanofluid potentials as a working fluid. It is impinged from a single-free 2 mm jet to reveal the thermal performance of such an arrangement experimentally under constant heat flux. The following are conclusions from the experimentations

1. The CuO–Cu/water nanofluid exhibits a very good enhancement in heat transfer, where the gained heat amount represented by Nusselt number was found to be 2.8% (in comparison with deionized water) at $\phi = 1\%$ and Re = 15,000, while the minimum gain in the heat was found to be 0.93% at $\phi = 0.2\%$ and Re = 5,000.
2. It was inferred that the enhancement in heat increases as the nozzle-to-plate spacing increases until a specific value of $H = 4$; thereafter, the increase in H spacing leads to a decrease in heat transfer.
3. Excessive increase in CuO–Cu nanoparticle concentration causes more pumping power consumption.
4. A CuO–Cu nanoparticles residual layer is formed at high CuO–Cu concentration which acts as an insulation layer that hinders the heat exchange.

Due to the lack of current similar objectives in the literature, and based on the limitations of this study, a specific range of Reynolds numbers and nanoparticles type were considered, while other limitations should be employed in the future studies.

Nomenclatures

A	area of the nozzle exit
A_t	the surface area of the target plate

C_p	heat capacity
h	heat Transfer Coefficient
I	electric current
k	thermal Conductivity
$\dot{m}$	mass flow rate
Nu	Nusselt Number
Pr	Prandtl Number
Q	volumetric flow rate
q	supplied electric power
Re	Reynold's number
T	temperature
t	target plate thickness
u	fluid velocity at the nozzle exit
V	voltage
Z	nozzle-to-target plate distance

Conflict of interest: Authors state no conflict of interest.

References

[1] Balla HH, Hashem AL, Kareem ZS, Abdulwahid AF. Heat transfer potentials of ZnO/water nanofluid in free impingement jet. Case Stud Therm Eng. 2021;27:101143.

[2] Gao F, Chen Y, Cai J, Ma C. Experimental study of free-surface jet impingement heat transfer with molten salt. Int J Heat Mass Transf. 2020;149:119160.

[3] Saha SK, Tiwari M, Sunden B, Wu Z. Advances in heat transfer enhancement. Switzerland: Springer International Publishing AG; 2016.

[4] Saha SK, Ranjan H, Emani MS, Bharti AK. Introduction to enhanced heat transfer, springerbriefs in applied sciences and technology. Switzerland: Springer International Publishing AG; 2019.

[5] Kareem ZS, Mohd Jaafar MN, Lazim TM, Abdullah S, Abdulwahid AF. Passive heat transfer enhancement review in corrugation. Exp Therm Fluid Sci. 2015;68:22–38.

[6] Sun B, Qu Y, Yang D. Heat transfer of single impinging jet with Cu Nanofluids. Appl Therm Eng. 2016;102:701–7.

[7] Amjadiana M, Safarzadeha H, Bahiraeib M, Nazaria S, Jaberia B. Heat transfer characteristics of impinging jet on a hot surface with constant heat flux using Cu_2O–water nanofluid: An experimental study. Int Commun Heat Mass Transf. 2020;112:104509.

[8] Sorour MM, El-Maghlany WM, Alnakeeb MA, Abbass AM. Experimental study of free single jet impingement utilizing high concentration SiO_2 nanoparticles water base nanofluid. Appl Therm Eng. 2019;160:114019.

[9] Wongcharee K, Chuwattanakul V, Eiamsa-ard S. Influence of CuO/water nanofluid concentration and swirling flow on jet impingement cooling. Int Commun Heat Mass Transf. 2017;88:277–83.

[10] Li Q, Xuan Y, Yu F. Experimental investigation of submerged single jet impingement using Cu–water Nanofluid. Appl Therm Eng. 2012;36:426–33.

[11] Nguyen CT, Galanis N, Polidori G, Fohanno S, Popa CV, Bechec AL. An experimental study of a confined and submerged impinging jet heat transfer using Al_2O_3-water nanofluid. Int J Therm Sci. 2009;48:401–11.

[12] Tie P, Li Q, Xuan Y. Heat transfer performance of Cu–water nanofluids in the jet arrays impingement cooling system. Int J Therm Sci. 2014;77:199–205.

[13] Eastman JA, Choi SUS, Li S, Yu W, Thompson LJ. Anomalously increased effective thermal conductivities of ethylene glycol-based nanofl uids containing copper nanoparticles. Appl Phys Lett. 2001;78:718–20.

[14] Paul G, Philip J, Raj B, Das PK, Manna I. Synthesis, characterization, and thermal property measurement of nano-Al95Zn05 dispersed nanofl uid prepared by a two-step process. Int J Heat Mass Tran. 2011;54:3783–8. doi: 10.1016/j.ijheatmasstransfer.2011.02.044

[15] Li Y, Zhou J, Tung S, Schneider E, Xi S. A review on development of nanofluid preparation and characterization. Powder Technol. 2009;196(2):89–101.

[16] Barewar SD, Tawri S, Chougule SS. Heat transfer characteristics of free nanofluid impinging jet on flat surface with different jet to plate distance: an experimental investigation. Chem Eng Process Process Intensif. 2019;136:1–10.

[17] Rahman A, Ismail A, Jumbianti D, Magdalena S, Sudrajat H. Synthesis of copper oxide nano particles by using phormidium cyanobacterium. Indonesian J Chem. 2009;9(3):355–60.

[18] Raykar VS, Singh AK. Thermal and rheological behavior of acetylacetone stabilized ZnO nanofluids. Thermochim Acta. 2010;502:60–5.

[19] Kareem ZS, Balla HH, AbdulWahid AF. Heat transfer enhancement in single circular impingement jet by CuO-water nanofluid. Case Stud Therm Eng. 2019;15:100508.

[20] Modak M, Chougule SS, Sahu SK. An experimental investigation on heat transfer characteristics of Hot surface by using CuO – water nanofluids in Circular jet impingement cooling. J Heat Transf. 2018;140:1–10.

[21] Coleman HW, Steele WG. Engineering application of experimental uncertainty analysis. AIAA J. 1995;33(10):1888–96.

[22] Sun B, Zhang Y, Yang D, Li H. Experimental study on heat transfer characteristics of hybrid nanofluid impinging jets. Appl Therm Eng. 2019;151:556–66.

[23] Barewar SD, Tawri S, Chougule SS. Heat transfer characteristics of free nanofluid impinging jet on flat surface with different jet to plate distance: An experimental investigation. Chem Eng Process Process Intensif. 2019;136:1–10.

[24] Han SH, Park HJ, Kim YH, Lee DH. The effects of thermal boundary conditions on the heat transfer characteristics of laminar flow in milli-scale confined impinging slot jets. Int J Heat Mass Transf. 2021;168:120865.

[25] Webb BW, Ma CF. Single-phase liquid jet impingement heat transfer. Adv Heat Transf. 1995;26(8):105–217.

[26] Lv J, Hu C, Zeng K, Bai M, Chang S, Gao D. Experimental investigation of free single jet impingement using SiO_2 -water nanofluid. Exp Therm Fluid Sci. 2017;84:39–46.